A Joint Linearity-Efficiency Model of Radio Frequency Power Amplifiers

Harald Enzinger*†, Karl Freiberger*† and Christian Vogel*‡
*Signal Processing and Speech Communication Laboratory, Graz University of Technology, Austria
†Telecommunications Research Center Vienna (FTW), Austria
‡FH Joanneum - University of Applied Sciences, Austria
Email: enzinger@tugraz.at, freiberger@tugraz.at, c.vogel@ieee.org

***Abstract*—We present an analytical model of the joint linearity-efficiency behavior of radio frequency power amplifiers. The model is derived by Fourier series analysis of a generic amplifier circuit including both strong nonlinearity due to current-clipping as well as weak nonlinearity due to transconductance variation. By selection of the biasing point, common amplifier classes like class A, class B and class AB can be modeled. For numerical evaluation, the model reduces to two lookup-tables, which makes it well suited for high-level system simulations. In an application example we demonstrate how the model can be used to simulate the error-vector-magnitude and the average efficiency for specific single-carrier and multi-carrier modulation schemes.**

I. Introduction

There is a practical trade-off between the linearity and the efficiency of radio frequency power amplifiers [1]. Since both linearity and efficiency are important performance indicators, the optimization [2] of this trade-off is of great interest for the design of wireless communication systems. With respect to linearity, many behavioral models have been proposed over the last decades [3] but none of them models efficiency. Just recently there have been several works [4]–[7] that address this issue by extending linearity models by efficiency models. These works demonstrate high modeling accuracy, but require parameter extraction from measurements. In some cases, however, such parameter extraction is not possible like in early phases of the system design. In other cases it is more desirable to have a generic power amplifier model instead of a specific one. For these purposes, previous works [8], [9] used a combination of simple memoryless linearity models and ideal class A or class B efficiency models. An advantage of this approach is that for some cases, the linearity-efficiency trade-off can be investigated analytically [8]. However, using two separate models for linearity and efficiency requires an additional assumption on how these models relate to each other. Additionally [8] and [9] only consider class A and class B but do not include the important case of class AB.

In the present paper, we present a mathematical model that jointly models the linearity and efficiency of radio frequency power amplifiers. This way the trade-off between these two properties can be modeled in a more natural way, giving additional insight into the cause of this trade-off.

The research leading to these results has received funding from the FFG Competence Headquarter program under the project number 4718971.

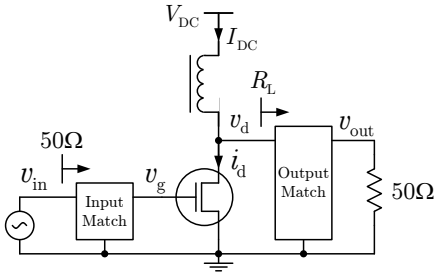

Fig. 1. Circuit model of a radio frequency power amplifier.

II. Circuit Model

For our analysis we use the circuit model of Fig. 1 which is also extensively used in [10]. It consists of a transistor, input and output matching networks, and a fixed supply attached to the drain of the transistor by an RF choke. Due to the inductive coupling between drain and supply, the drain node v_{d} is biased at V_{DC}. The biasing of the input node is not explicitly shown but we will assume that the gate node v_{g} can be set to an arbitrary DC voltage. For the large-signal transistor behavior we assume a voltage-controlled current source with a nonlinear i_{d} over v_{g} characteristic as in the left plot in Fig. 2. The drain current i_{d} is zero for gate voltages v_{g} below the threshold voltage V_{th} and increases with v_{g} until the saturation voltage V_{sat} is reached where it remains at I_{max}. In the right plot in Fig. 2, the waveform of i_{d} resulting from a large sinusoidal input signal is shown. This waveform is a distorted version of the input signal and we can discriminate between two types of nonlinearity: Strong nonlinearity due to current-clipping below zero and above I_{max} and weak nonlinearity due to transconductance variation between V_{th} and V_{sat}.

In the conventional efficiency analysis [8]–[10], the weak nonlinearity is neglected and class A or class B is considered. For class A this leads to a peak efficiency of 50% which decreases quadratically with reduced input magnitude and for class B it leads to a peak efficiency of $\frac{4}{\pi} \approx 78.5\%$ which decreases linearly with reduced input magnitude. Neglecting the weak nonlinearity is reasonable with respect to efficiency, but it results in perfect linearity for class A and class B which is too simplistic. To get a more realistic model of the joint linearity and efficiency behavior we will proceed with an analysis that considers both strong and weak nonlinearities.

978-1-4799-5341-7/16/$31.00 ©2016 IEEE

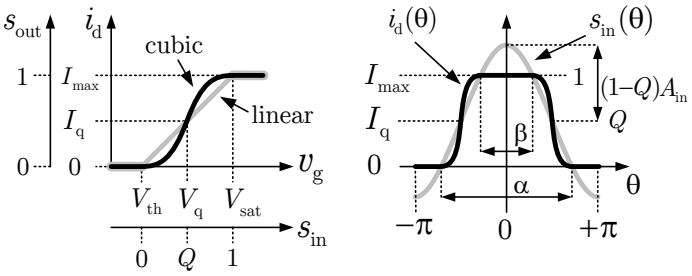

Fig. 2. Left: i_{d} over v_{g} characteristics. Right: Waveforms of normalized input signal $s_{\text{in}}(\theta)$ and drain current $i_{\text{d}}(\theta)$ using the cubic i_{d} over v_{g} model.

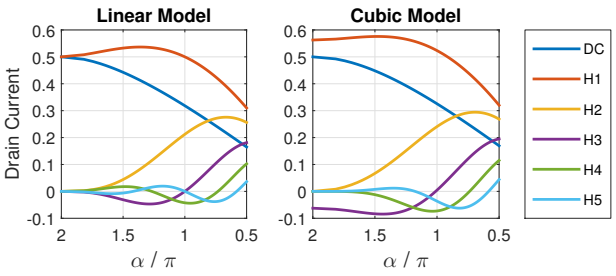

Fig. 3. Normalized spectral components of drain current i_{d} over conduction angle α for $A_{\text{in}} = 1$ showing $I_{\text{DC}}/I_{\text{max}}$ (DC) and I_k/I_{max} (H1-H5).

III. Analysis

A. Mathematical Representation

For mathematical simplicity we introduce normalized units for the input signal according to axis s_{in} in the left plot in Fig. 2. Using these units we define the input signal by

$$s_{\text{in}}(\theta) = Q + (1 - Q)A_{\text{in}} \cos(\theta) \tag{1}$$

with Q being the quiescent point, A_{in} being the input amplitude and θ being an angle in radian representing the progress in time. Note that by definition $A_{\text{in}} = 1$ represents the input magnitude where the peaks of v_{g} reach V_{sat} and the peaks of i_{d} reach I_{max}, independent of the quiescent point Q.

To describe the weak nonlinearity of the i_{d} over v_{g} characteristic between V_{th} and V_{sat}, we use the cubic model

$$s_{\text{out}}(\theta) = 3s_{\text{in}}^2(\theta) - 2s_{\text{in}}^3(\theta) \tag{2}$$

which is physically justified for MOSFET transistors, since it shows square-law behavior near V_{th} and a continuous saturation near V_{sat}. This model was initially proposed in [10], but only for illustration, not for linearity or efficiency analysis. Note that the simple form of (2) is facilitated by the normalization of s_{in}, i.e., a representation in v_{g} would also include terms of degree 0 and 1. Also note that (2) represents an instantaneous nonlinearity applied to an RF signal which should not be confused with a polynomial baseband model that describes the mapping between complex envelopes [11].

To describe the strong nonlinearity due to current-clipping, we define the conduction angle α and the saturation angle β according to the right plot in Fig. 2. This allows the definition of the drain current waveform over one period by

$$i_{\text{d}}(\theta) = \begin{cases} I_{\text{max}} & 0 < |\theta| \leq \frac{\beta}{2}, \\ I_{\text{max}} s_{\text{out}}(\theta) & \frac{\beta}{2} < |\theta| \leq \frac{\alpha}{2}, \\ 0 & \text{otherwise.} \end{cases} \tag{3}$$

To jointly analyze the linearity and efficiency, we will first derive a Fourier series representation of the drain current i_{d} and then relate the DC and first harmonic current components to the DC power consumption and the RF output power.

B. Fourier Series of Drain Current

The Fourier series of the drain current is given by

$$i_{\text{d}}(\theta) = I_{\text{DC}} + \sum_{k=1}^{\infty} I_k \cos(k\theta) \tag{4}$$

with the harmonic current amplitudes given by

$$I_k = \frac{2}{\pi} \int_0^{\pi} i_{\text{d}}(\theta) \cos(k\theta)\, d\theta. \tag{5}$$

Inserting (3) into (5) leads to

$$I_k = \frac{2}{\pi} \left[\int_0^{\frac{\beta}{2}} I_{\text{max}} \cos(k\theta)\, d\theta + \int_{\frac{\beta}{2}}^{\frac{\alpha}{2}} I_{\text{max}} s_{\text{out}}(\theta) \cos(k\theta)\, d\theta \right] \tag{6}$$

which is further evaluated by moving I_{max} to the left and inserting the definitions from (1) and (2) leading to

$$\begin{aligned} \frac{I_k}{I_{\text{max}}} = \frac{2}{\pi} \Bigg[& \int_0^{\frac{\beta}{2}} \cos(k\theta)\, d\theta \\ & + \left[3Q^2 - 2Q^3\right] \int_{\frac{\beta}{2}}^{\frac{\alpha}{2}} \cos(k\theta)\, d\theta \\ & + \left[6Q - 6Q^2\right] \left[1 - Q\right] A_{\text{in}} \int_{\frac{\beta}{2}}^{\frac{\alpha}{2}} \cos(\theta) \cos(k\theta)\, d\theta \\ & + \left[3 - 6Q\right] \left[1 - Q\right]^2 A_{\text{in}}^2 \int_{\frac{\beta}{2}}^{\frac{\alpha}{2}} \cos^2(\theta) \cos(k\theta)\, d\theta \\ & - 2\left[1 - Q\right]^3 A_{\text{in}}^3 \int_{\frac{\beta}{2}}^{\frac{\alpha}{2}} \cos^3(\theta) \cos(k\theta)\, d\theta \Bigg]. \end{aligned} \tag{7}$$

Although (7) looks rather complicated, it can be evaluated efficiently, since closed-form solutions exist for the integrals. For further details concerning numerical evaluation please see the Matlab code [12] which also includes the mapping of A_{in} and Q to α and β as well as the linear model that neglects weak nonlinearity between V_{th} and V_{sat}. A comparison of the resulting spectral components for the linear and the cubic model is shown in Fig. 3. Significant differences can be observed for the first and third harmonic in the class A ($\alpha = 2\pi$) and class AB ($2\pi > \alpha > \pi$) operation regions.

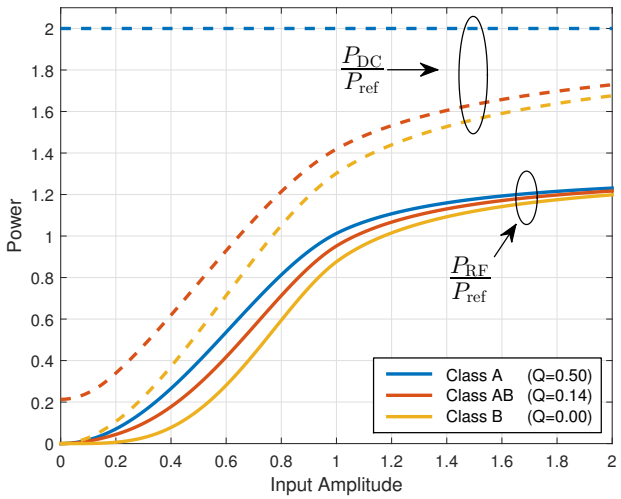

Fig. 4. Normalized DC power consumption and RF output power over input amplitude A_{in} for various operation modes set by quiescent point Q.

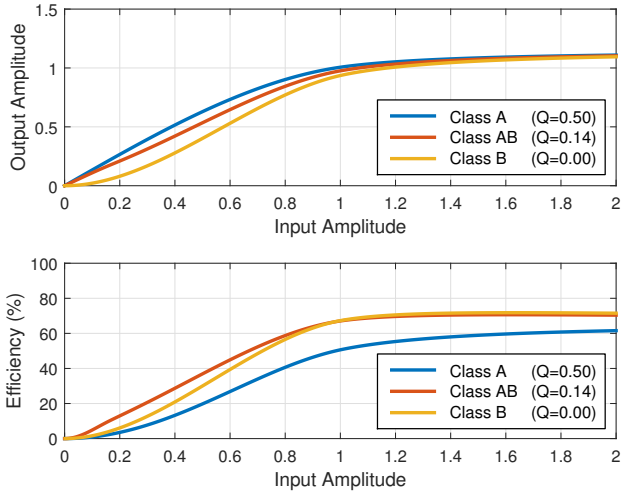

Fig. 5. Top: Linearity in terms of AM-AM characteristic showing amplitude A_{out} over amplitude A_{in}. Bottom: Instantaneous efficiency η_{inst} over A_{in}.

C. From Drain Current To DC and RF Power

For a simple relation between drain current and DC and RF powers, two assumptions are required. The first assumption is that the output matching network implements a defined impedance at the first harmonic and an ideal short at all higher harmonics. As a consequence, the RF output power is solely defined by the first harmonic current and higher harmonic currents are dissipated as heat by the transistor. The second assumption is that the output of the transistor shows ideal current-source behavior without feedback from the drain voltage to the drain current, i.e. the transistor output conductance g_{ds} and the knee voltage V_{k} are zero.

To get normalized powers we first define a reference power. We set this reference to the RF output power in class A operation with maximum signal swing such that no current or voltage clipping occurs. In this mode, the amplitude of the first harmonic current is equal to the quiescent current of $0.5\,I_{\mathrm{max}}$ and the amplitude of the output voltage is equal to the DC level of the drain node which is V_{DC}. The reference power is the product of these amplitudes divided by two resulting in

$$P_{\mathrm{ref}} = \frac{V_{\mathrm{DC}} I_{\mathrm{max}}}{4}. \tag{8}$$

To realize this output power, the impedance of the matching network at the first harmonic must be set to the ratio of these amplitudes, known as a load-line match [10], resulting in

$$R_{\mathrm{ref}} = \frac{V_{\mathrm{DC}}}{0.5 I_{\mathrm{max}}}. \tag{9}$$

The DC power consumption is $P_{\mathrm{DC}} = V_{\mathrm{DC}} I_{\mathrm{DC}}$ which, after normalization by (8) gives

$$\frac{P_{\mathrm{DC}}}{P_{\mathrm{ref}}} = 4 \frac{I_{\mathrm{DC}}}{I_{\mathrm{max}}} \tag{10}$$

The RF output power is $P_{\mathrm{RF}} = \frac{1}{2} I_1^2 R_{\mathrm{L}}$ with R_{L} being the actual load resistance of the matching network at the first harmonic. Normalizing P_{RF} by (8) and R_{L} by (9) gives

$$\frac{P_{\mathrm{RF}}}{P_{\mathrm{ref}}} = 4 \left(\frac{I_1}{I_{\mathrm{max}}} \right)^2 \frac{R_{\mathrm{L}}}{R_{\mathrm{ref}}}. \tag{11}$$

For class A operation with the linear transistor model, the actual load resistance R_{L} that implements a load-line match is equal to the reference resistance R_{ref} by definition. For other operation modes or transistor models this is not the case. From Fig. 3 it can be seen that for the cubic transistor model, the first harmonic current is slightly higher than $0.5\,I_{\mathrm{max}}$ throughout the complete class AB operation range. To avoid voltage clipping, we therefore use a reduced load resistance of $R_{\mathrm{L}}/R_{\mathrm{ref}} = 0.8$ for our evaluations. In Fig. 4 the resulting power values, swept over the input amplitude A_{in} are shown.

D. Linearity and Efficiency

The power characteristics of Fig. 4 contain all information we need to evaluate linearity and efficiency. To visualize this more explicitly, we define two new variables. First we define the normalized output amplitude

$$A_{\mathrm{out}} = \sqrt{\frac{P_{\mathrm{RF}}}{P_{\mathrm{ref}}}} \tag{12}$$

which must be normalized, since gain is not part of our model. Second, we define the instantaneous efficiency

$$\eta_{\mathrm{inst}} = \frac{P_{\mathrm{RF}}}{P_{\mathrm{DC}}}. \tag{13}$$

In Fig. 5 both A_{out} and η_{inst} are plotted as functions of the input amplitude A_{in}. From this plot we can see that in class AB operation, high linearity and efficiency can be achieved which makes this mode especially important in practice. The high linearity of class AB can be explained by a cancellation of weak and strong nonlinearity at a given quiescent point which is known as the sweet spot [10].

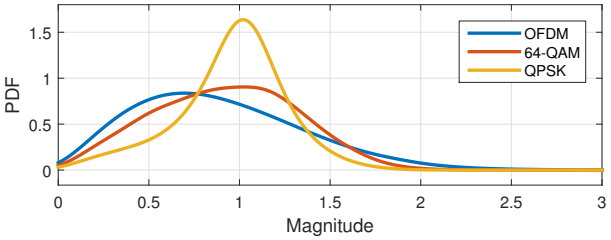

Fig. 6. Probability density functions (PDF) of the signal envelope for various modulation schemes, normalized to a root-mean-square magnitude of one.

IV. Application Example

In the following example we show how the proposed model can be used to analyze the linearity-efficiency trade-off with respect to specific modulation schemes. As linearity metric we use the error vector magnitude (EVM) which is the mean-square-error between the transmitted and received symbols. As efficiency metric, we use the average efficiency defined by

$$\eta_{\mathrm{avg}} = \frac{\mathrm{E}\{P_{\mathrm{RF}}\}}{\mathrm{E}\{P_{\mathrm{DC}}\}} \tag{14}$$

with $\mathrm{E}\{\cdot\}$ being the expectation operator. For practical signals, which are ergodic, the expectations in (14) can be evaluated either in the time-domain or in the ensemble-domain. However, it is important that the numerator and the denominator in (14) are evaluated separately, since in general $\eta_{\mathrm{avg}} \neq \mathrm{E}\{\eta_{\mathrm{inst}}\}$.

We use three modulation schemes for our example, which are orthogonal frequency-division multiplexing (OFDM), single-carrier quadrature amplitude modulation (64-QAM) and single-carrier quadrature phase shift keying (QPSK). The setup of the OFDM modulation is similar to the 802.11 WLAN physical layer and due to the large number of subcarriers, the results are independent of the symbol constellation. For the single-carrier modulations we use root-raised-cosine transmit and receive filters with a roll-off factor of 0.1. A plot of the corresponding envelope distributions is shown in Fig. 6.

To evaluate the linearity and efficiency we first generate sufficiently long realization of the respective signals in complex baseband representation. Then we send these signals through the power amplifier model which consists of the lookup tables of RF output power and DC power consumption shown in Fig. 4. This gives the complex output signals and the instantaneous RF and DC power signals. Finally, we calculate the EVM from the complex output signals and the average efficiency from the instantaneous RF and DC power signals. Repeating this for various backoff levels, with and without digital predistortion (DPD), leads to the results in Fig. 7.

An important observation from Fig. 7 is that the average efficiency is mainly defined by the required backoff, since variations of the envelope PDF due to signal type or digital predistortion have only little impact on the average efficiency. We can also see from Fig. 7, that OFDM is most sensitive to nonlinear distortion. It requires a relatively large backoff which leads to low average efficiency. If digital predistortion is used, the backoff can be reduced which increases the efficiency.

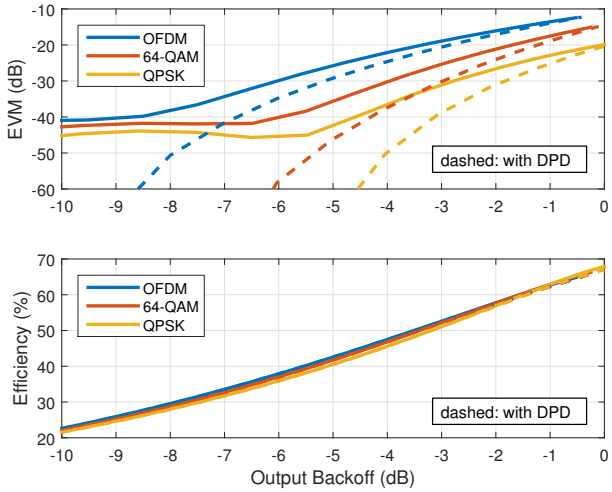

Fig. 7. Error vector magnitude (EVM) and average efficiency η_{avg} over output backoff from P_{ref} for class AB amplifier model with $Q = 0.14$.

V. Conclusion

We presented a joint linearity-efficiency model of radio frequency power amplifiers. Using this model, we demonstrated how the linearity-efficiency trade-off can be evaluated for various modulation schemes. In future work, the model may also be applied to evaluate new transmitter architectures. A Matlab implementation of the model is available [12].

References

[1] P. Lavrador, T. Cunha, P. Cabral *et al.*, "The linearity-efficiency compromise," *IEEE Microwave Magazine*, vol. 11, no. 5, pp. 44–58, 2010.

[2] K. Freiberger, M. Wolkerstorfer, H. Enzinger *et al.*, "Digital predistorter identification based on constrained multi-objective optimization of WLAN standard performance metrics," in *IEEE Int. Symp. on Circuits and Systems (ISCAS)*, 2015, pp. 862–865.

[3] M. Isaksson, D. Wisell, and D. Ronnow, "A comparative analysis of behavioral models for RF power amplifiers," *IEEE Trans. Microw. Theory Tech.*, vol. 54, no. 1, pp. 348–359, 2006.

[4] J. Pedro, P. Cabral, T. Cunha *et al.*, "A multiple time-scale power amplifier behavioral model for linearity and efficiency calculations," *IEEE Trans. Microw. Theory Tech.*, vol. 61, no. 1, pp. 606–615, 2013.

[5] S. Glock, B. Sogl, P. Vizaretta *et al.*, "An extension of power amplifier behavioral models for optimizing battery current at system level," in *IEEE Topical Conference on Power Amplifiers for Wireless and Radio Applications (PAWR)*, 2013, pp. 67–69.

[6] S. Glock, J. Rascher, B. Sogl *et al.*, "A novel power amplifier behavioral model for improving the linearity-efficiency tradeoff," in *IEEE MTT-S International Microwave and RF Conference*, 2013, pp. 1–4.

[7] O. Hammi, "Low complexity behavioral model for RF power amplifiers' linearity and efficiency prediction," in *IEEE International RF and Microwave Conference (RFM)*, 2013, pp. 283–286.

[8] H. Ochiai, "An analysis of band-limited communication systems from amplifier efficiency and distortion perspective," *IEEE Transactions on Communications*, vol. 61, no. 4, pp. 1460–1472, 2013.

[9] H. Yu, C. Kok, and G. Wei, "Power efficiency optimization of OFDM systems in the presence of nonlinear distortion," in *International Conference on Communications, Circuits and Systems*, 2006, pp. 1245–1250.

[10] S. C. Cripps, *RF power amplifiers for wireless communications*, 2nd ed. Artech House, 2006.

[11] H. Enzinger, K. Freiberger, and C. Vogel, "Analysis of even-order terms in memoryless and quasi-memoryless polynomial baseband models," in *IEEE Int. Symp. on Circuits and Systems (ISCAS)*, 2015, pp. 1714–1717.

[12] H. Enzinger, "Joint Linearity-Efficiency Model," Matlab File Exchange: www.mathworks.com/matlabcentral/fileexchange/53413, 08 Oct 2015.